Demonstration of a Hybrid FSO/VLC Link for the Last Mile and Last Meter Networks

Petr Pesek
Stanislav Zvánovec
Petr Chvojka
Zabih Ghassemlooy
Paul Anthony Haigh
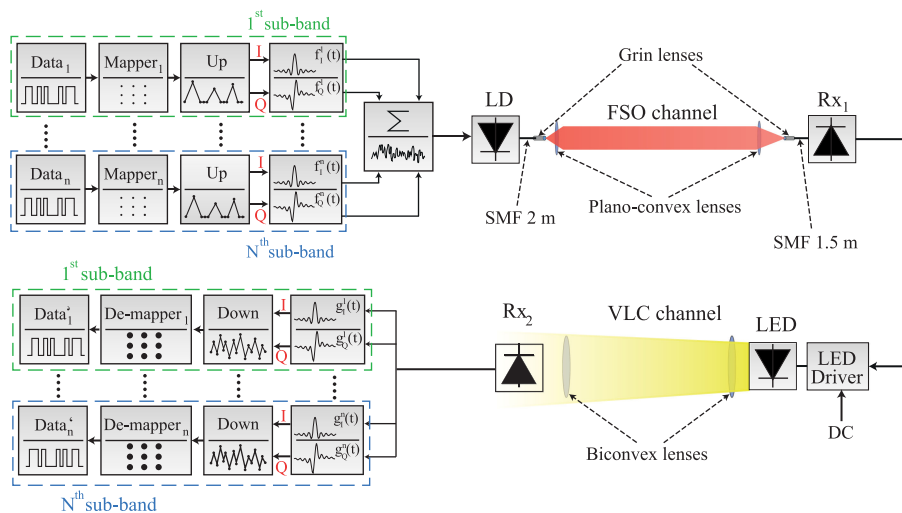
Demonstration of a Hybrid FSO/VLC Link for the Last Mile and Last Meter Networks

Petr Pesek [1], **Stanislav Zvánovec** [1], **Petr Chvojka** [1], **Zabih Ghassemlooy** [2] **and Paul Anthony Haigh** [3]

[1]Department of Electromagnetic Field, Faculty of Electrical Engineering, Czech Technical University in Prague, Prague 16627, Czech Republic
[2]Optical Communications Research Group, NCRLab, Faculty of Engineering and Environment, Northumbria University, Newcastle upon Tyne NE1 8ST, U.K.
[3]Department of Electronic and Electrical Engineering, University College London, London WC1E 6BT, U.K.

Abstract: In this paper, a hybrid free-space optical and visible light communication (FSO/VLC) system was experimentally demonstrated as a solution to overcome the last mile and last meter access networks bandwidth bottleneck. We evaluate the system performance of a multiband carrier-less amplitude and phase (m-CAP) modulation scheme for a range of FSO/VLC link lengths and m-CAP parameters (i.e., the roll-off factor of the filters and a number of subcarriers) in terms of the data rate R_b (i.e., spectral efficiency). We show that for the configuration with a 1-m VLC link the 10-CAP offers more than a 40% improvement in the measured R_b compared to 2-CAP for the same bit error rate target. The R_b penalty due to the extension of a VLC-link span from 1 to 3 m reaches to 12.6 Mb/s for the 10-CAP scheme (i.e., ~39% degradation in R_b). To fully cover all aspects of the hybrid FSO/VLC system, we also investigate the atmospheric turbulence effect on the 500-m FSO link where R_b is decreased by 30% for the refractive index structure parameter C_n^2 of 2.4×10^{-15} m$^{-2/3}$ compared to a clear channel condition.

Index Terms: Visible light communication, free space optics, multiband carrier-less amplitude and phase modulation.

1. Introduction

Due to an increasing number of mobile users, video streaming, the deployment of technologies such as the Internet of Things (IoT) and the end-user's demand for high-quality services requiring enormous transmission capacity, is growing exponentially [1]. Although advances made in radio frequency (RF) technologies have been able to address challenges posed by this unprecedented data growth, the available RF spectrum is rapidly becoming congested to saturation. Therefore, both the commercial sector and academia have actively begun investigating wireless technologies to complement to RF systems. Optical wireless communication (OWC) technologies offer unregulated bandwidth (in the order of THz) which is compatible with existing high-speed backbone optical fiber communication networks. As a part of OWC, the mature free space optical (FSO) communications

system, which mostly operates in the infrared band, is a promising solution to overcome the bandwidth bottleneck in outdoor last mile access networks, particularly in extremely dense urban areas, where the installation of optical fiber infrastructure is cost-ineffective [2]. FSO systems are, in most cases, intended for line-of-sight (LOS) applications offering similar features as to single-mode fibers (SMFs), including a comparable bandwidth, security, low installation cost and immunity to RF-induced electromagnetic interference [3]. Nowadays, FSO systems with data rates R_b up to 10 Gb/s are commercially available [4] and up to Tb/s have been demonstrated for laboratory-based links [5]. However, as with RF technologies, FSO link performance is influenced by atmospheric channel conditions such as turbulence, fog, smog, etc. Under clear weather conditions, atmospheric turbulence is the main source of random fluctuations in both the phase and intensity of the received optical signal [6].

In the visible spectrum, OWC technology is best known as visible light communications (VLC), which is, at present, is mostly intended for short range indoor applications, i.e., last meter access networks. The main feature of VLC is that it uses light emitting diode (LED)-based light sources for illumination, high-speed data communications and highly-accurate indoor localization [4], [7]. However, in VLC systems the main bottleneck is the LED bandwidth B_{LED}, which is around 3 MHz for white phosphorus [8], and 20+ MHz for RGB (red, green and blue) LEDs [9], which is not sufficient to achieve high R_b over a typical link span of a few meters.

To address this issue, a number of options have been proposed and reported in the literature including *(i)* equalization schemes [7]; *(ii)* multilevel modulations [10]; *(iii)* micro-LEDs with higher B_{LED} [11]; and *(iv)* multi-carrier modulation schemes, such as orthogonal frequency division multiplexing (OFDM) and carrier-less amplitude and phase (CAP) modulation [12]–[17]. Note, OFDM supports higher order modulation formats, such as quadrature amplitude modulation (QAM) as well as other features including adaptive power and bit-loading algorithms while also overcoming multipath induced intersymbol interference (ISI) [12]. However, the main drawback of OFDM is the high peak-to-average power ratio (PAPR), which can result in signal clipping and, therefore, distortion due to the nonlinear characteristics of LEDs and amplifiers [13]. The CAP scheme is very similar to QAM in terms of transmitting two parallel streams of data using only two filters with orthogonal waveforms (i.e., quadrature and in-phase), albeit that it does not rely on a local oscillator to generate the carrier signals. CAP offers a number of advantages including: *(i)* reduced computational complexity, which depends on the length of finite impulse response (FIR) filters used at the transmitter (Tx) and the receiver (Rx); *(ii)* the same spectral efficiency η_s and performance as QAM; and *(iii)* flexibility in design, since it is possible to use both analogue and digital filters to generate the signal. CAP was experimentally demonstrated to outperform OFDM in terms of R_b (i.e., spectrum efficiency) by $\sim$20% over the same transmission link [14].

The first experimental FSO/VLC heterogeneous interconnection was presented in [18] where the authors demonstrated OFDM with data aggregation. In this paper, we have focused on the proof of concept of a hybrid FSO/VLC link with multiband CAP (m-CAP) for the last mile and last meter access networks. The emphasis is on experimental evaluation of the system performance under atmospheric conditions when considering parameters such as the roll-off factor β for the set of m and their influence, on the measured R_b for a range of transmission spans. Note, we have used a moderate R_b of 40 Mb/s and short transmission spans for both FSO and VLC links, which can be readily increased for higher Rb and longer link distances. The results demonstrate the potential of the hybrid FSO/VLC link as an alternative solution to overcome the bandwidth bottleneck in the last mile and last meter access networks, see Figure 1. Note that, the inter-building connectivity is realized by a high-speed FSO link, which can feed a number of access points in indoor environments. The received FSO signal is then distributed via SMFs within rooms and the VLC technology is used to provide the last meter connectivity for the end users.

The paper is organized as follows: in Section 2, the experimental setup and system parameters are briefly outlined, whereas in Section 3, the results of hybrid FSO/VLC link are shown. Finally, the conclusions are given in Section 4.
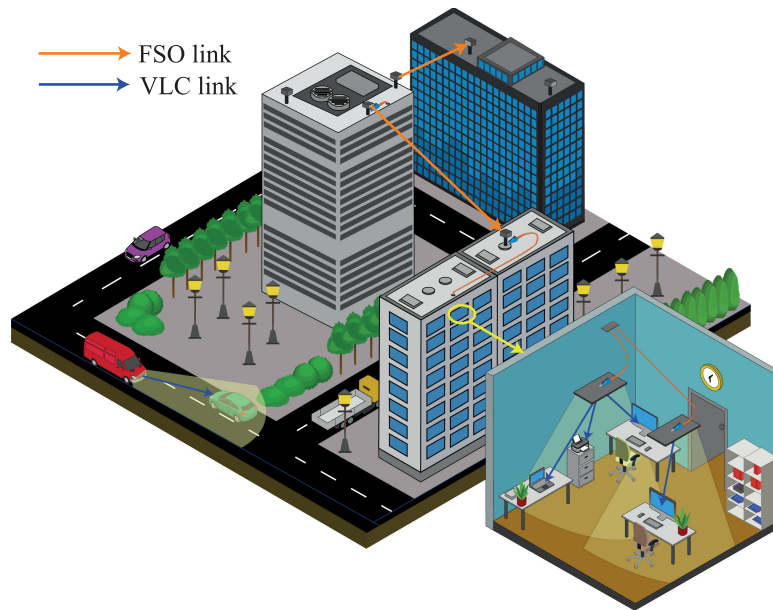
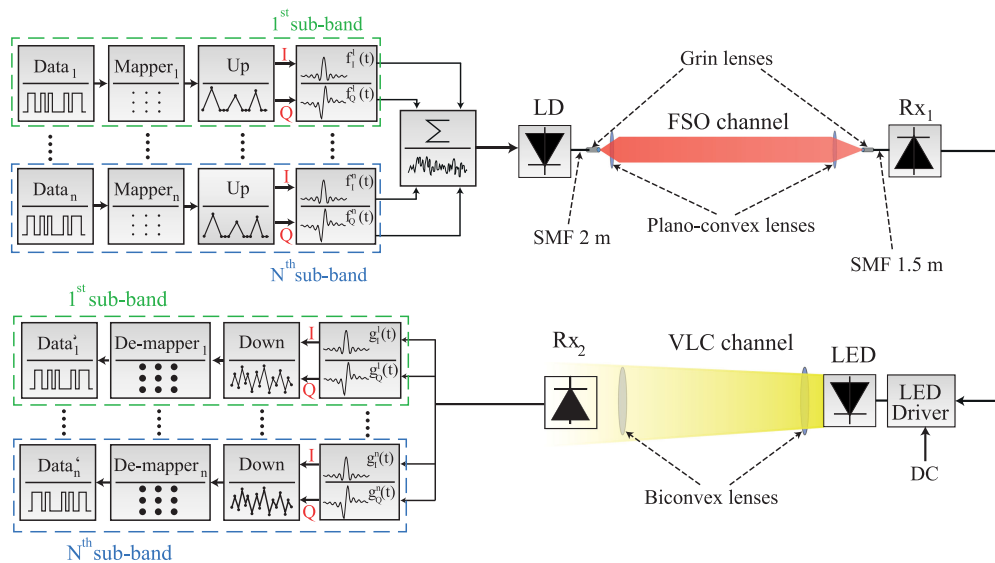Fig. 1. Scenario for last mile and last meter interconnections in urban area utilizing FSO and VLC links.

Fig. 2. Experimental setup for the hybrid FSO/VLC link. "Up", "Down" refers to up-sampling and down-sampling, respectively.

2. Experimental Setup

The performance of the proposed hybrid FSO/VLC link with m-CAP has been investigated utilizing the setup illustrated in Figure 2. A 2^{13-1} independent pseudorandom binary sequence generated for each subcarrier (SC) is mapped into M-QAM symbols where M is the order of QAM. The mapped signal is then up-sampled by zero padding, prior to being split into the in-phase I and the quadrature Q components, which are then applied to I and Q pulse shaping square-root-raised cosine (SRRC) filters, whose impulse responses form a Hilbert pair has been clearly documented in the literature [15]. The generated output signal is combined and loaded to a Rohde & Schwarz vector signal generator (SMW200A) for intensity modulation (IM) of a commercial laser diode (FITEL

FRL15DCW) operating at a wavelength of 1550 nm with an output power of 5 dBm. The output of the laser diode is launched into an SMF via a gradient-index (GRIN) lens (GRIN2315-Thorlabs). A plano-convex lens (Thorlabs N-BK7), with a focal length f_L of 100 mm, placed in front of the SMF, is used for the beam collimation for propagation over the free space channel. At the Rx, a plano-convex lens is employed to focus the optical beam via a SMF onto a photodetector whose output is amplified and applied to the LED driver with DC biasing prior to the IM of the LED. Note, the SMF is intended for signal distribution within a building. The insertion loss of the optical link (including pigtails, FSO channel and SMFs) is 15 dB at 1550 nm. For the VLC link, we used a commercially available LED (an OSRAM Golden Dragon with B_{LED} LED of 1 MHz) biased at ∼390 mA to ensure operation within its linear region [17]. We also used two biconvex lenses with $f_{L1} = 25$ mm and $f_{L2} = 35$ mm were used at the Tx and the Rx, respectively. An optical Rx (Thorlabs PDA10A) was used for the regeneration of the transmitted signal. The regenerated signal is resampled to the sampling frequency of the transmitted signal and passed through the time-reversed Rx filters, which are matched to the Tx filters. Following down-sampling and demodulation, the recovered M-QAM symbols are compared with the transmitted data for BER estimation. For this measurement, we set the transmitted signal bandwidth to 5 MHz. To achieve a maximum R_b, we used a pilot binary phase shift keying (BPSK) signal to load an appropriate number of bits/symbol to individual SC based on the measured signal to noise ratio (SNR). For the acquisition of received data, we used a real-time digital oscilloscope (1 GSa/s LeCroy WaveRunner Z640i) to capture the signal for offline processing (i.e., R_b and η_s) in the MATLAB domain. More details on the m-CAP adaptation can be found in [17].

3. Experimental Results

3.1 A Clear Atmosphere

In this section, the performance of the m-CAP based hybrid FSO/VLC link under a clear atmosphere, is presented. The complexity of the m-CAP scheme depends mainly on *(i)* the length of filters Ls; *(ii)* roll-factor β; and *(iii)* the number of SCs (i.e., m). Note, L_s is set to 10 symbols based on the results of our previous work on VLC [19] where we showed that for $L_s > 10$ there was only marginal performance improvement. Here, we therefore focus mainly on β and m. Note, for each increment of m we require 4 additional filters (2 each at the TX and the Rx). Results are presented in terms of R_b and η_s for a range of $m = \{2 - 10\}$ and $\beta = \{0.2, 0.4\}$.

In the first experiment, we measured R_b for a range of a VLC link span, m and β, as shown in Figure 3. The FSO transmission span was 2 m due to laboratory space, but the performance can be recalculated to that of the outdoor schemes with longer distance. The BER threshold level was set to 3.8×10^{-3} allowing the margin for the 7% forward error correction (FEC) overhead. Based on a flat response, the FSO link itself offers R_b of ∼40 Mb/s independent of the order of m-CAP. For a 1 m FSO/VLC link with $\beta = 0.2$, increasing m improves the measured R_b from 18.6 Mb/s to 32.4 Mb/s for 2 and 10-CAP, respectively, where the maximum R_b corresponds to η_s of 6.48 b/s/Hz. As it is clear from Figure 3, the link with $\beta = 0.4$ outperforms $\beta = 0.2$ for up to 3-CAP, due to the improved bandwidth allocation of the individual SCs, which are not degraded much by the LED's frequency response. With the VLC link span extension, R_b significantly decreases based on the lower SNR. For example, a 4 m VLC link achieves the maximal R_b of 20 Mb/s for 5-CAP and $\beta = 0.2$ and increasing m does not result in further performance improvement because of SNR degradation. Note, for VLC links of 2 m, 3 m and 4 m, R_b is reduced by 4.6 Mb/s, 7.2 Mb/s and 12.5 Mb/s, respectively compared to a 1 m 10-CAP VLC link with $\beta = 0.2$.

3.2 Atmospheric Turbulence Influence

Here we investigate the system performance considering the effect of atmospheric turbulence on the inter-building FSO link. We have used a dedicated indoor FSO testbed chamber and employed heating fans to create turbulence along the optical propagation path [20]. The turbulence level is
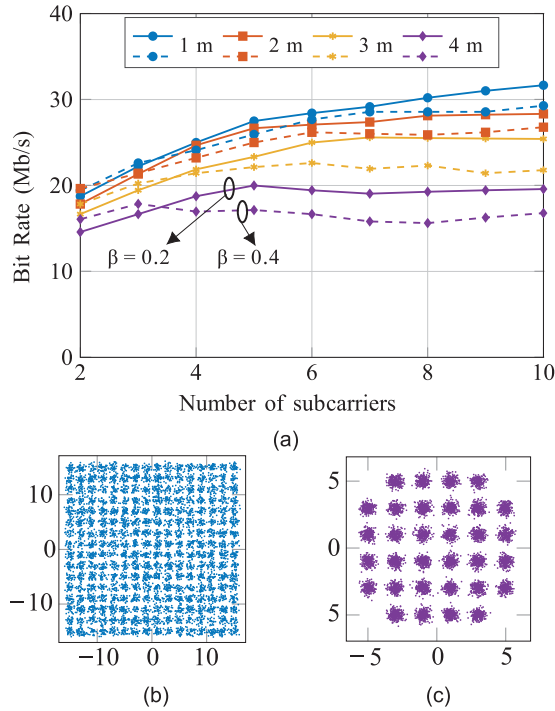
Fig. 3. (a) Experimentally measured data rates for several VLC link lengths and: $\beta = 0.2$ (solid) and 0.4 (dashed). Note, the constellation diagrams illustrate 3rd SCs for the 6-CAP scheme and $\beta = 0.2$ in case of VLC link is (b) 1 m and (c) 4 m long.

measured in the terms of refractive index structure parameter C_n^2 using 20 temperature sensors positioned at 0.1 m apart along the indoor FSO chamber. At higher levels of turbulence, the propagating optical wave experiences a higher level of intensity and phase fluctuations, which eventually leads to wider, scattered beam patterns at the Rx. This behavior is described by Kolmogrov's turbulence theory where the refractive index changes in the order of several parts per million for every 1 K atmospheric temperature variation [21]. Figure 4 shows the measured R_b as a function of m for the proposed hybrid FSO/VLC link (i.e., VLC and FSO channels of 2 m span each) for a range of turbulence levels (C_n^2). We have investigated the turbulence level up to $C_n^2 = 1.2 \times 10^{-10}$ m$^{-2/3}$ for a 2 m FSO under a laboratory conditions. Note, for higher turbulence levels and a short FSO link we can recalculate the C_n^2 value using Rytov variance [6] to obtain the turbulence levels for longer outdoor FSO links. The scintillation index is dependent on the value of (C_n^2) and the temperature gradient. Assuming a constant (C_n^2) over a short propagation span of ΔL_{in} and ΔL_{out} for an indoor and outdoor FSO links, respectively, the relation $R_{in/out}$ between the two is given by:

$$R_{in/out} = \frac{C_{n-out}^2}{C_{n-in}^2} \times \left(\frac{\Delta L_{out}}{\Delta L_{in}}\right)^{11/6} \tag{1}$$

Hence, to calibrate the FSO link performance in order to make the same as the outdoor link, $R_{in/out}$ should be unity. Note that, *(i)* link segmentation is used to keep the temperature gradient constant; and *(ii)* $C_{n-out}^2 < C_{n-in}^2$; *(iii)* $10^{-16} < C_{n-out}^2 < 10^{-14}$ m$^{-2/3}$ for the weak turbulence [22], [23]. Using (1) and for $C_{n-in}^2 \sim 1.2 \times 10^{-10}$ m$^{-2/3}$ as well as C_{n-out}^2 of 9.2×10^{-14} m$^{-2/3}$, $4,8 \times 10^{-15}$ m$^{-2/3}$, and 1.4×10^{-15} m$^{-2/3}$ outdoor FSO link spans are 100, 500 and 1000 m, respectively, which induces the same weak turbulence effect as the indoor link. However, by generating higher temperature gradients more than 7 °K/m in the indoor experimental FSO link we can achieve the same performance as the longer outdoor FSO link.

It can be seen that R_b reduces significantly with increasing turbulence levels. For instance, for 10-CAP and $\beta = 0.2$, the drops in R_b are 8.9% and 30% for $C_n^2 = 3.9 \times 10^{-17}$ m$^{-2/3}$ and
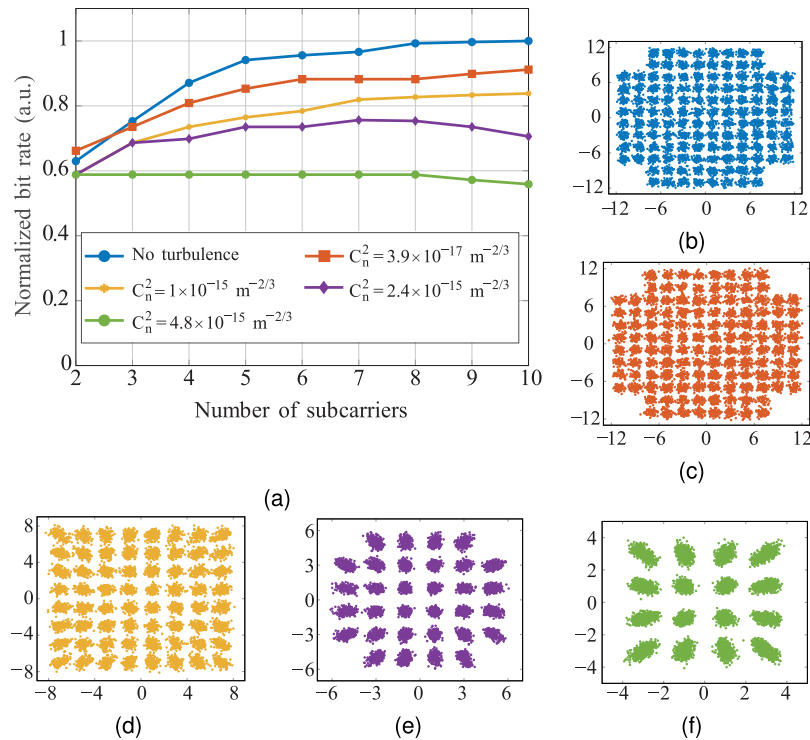
Fig. 4. (a) Measured hybrid FSO/VLC link data rate performance corresponds to the extended 500 m FSO link in the range of C_n^2 and $\beta = 0.2$. Note, the constellation diagrams: (b)–(f) illustrate 3rd SCs for the 6-CAP scheme with the colors corresponding to C_n^2.

$C_n^2 = 2.4 \times 10^{-15}$ m$^{-2/3}$, respectively compared to the link with no turbulence. As observed from the figure, for higher levels of turbulence (i.e., $C_n^2 = 9.2 \times 10^{-14}$ m$^{-2/3}$) the waveform distortion for a 500 m-long FSO link is considerably higher (see the constellation diagrams). Turbulence effect can be mitigated by increasing m for lower turbulence levels, e.g. for $C_n^2 = 3.9 \times 10^{-17}$ m$^{-2/3}$ an improvement in R_b of 25% was observed, while for higher turbulences ($C_n^2 = 2.4 \times 10^{-15}$ m$^{-2/3}$) increasing m does not lead to improvement in R_b.

4. Conclusion

A hybrid FSO/VLC system with m-CAP, suitable for a last mile and last meter access networks interconnected by a single mode fiber offering both security at the physical layer and a low installation cost, was presented in this paper. We showed that, comparing 2-CAP and 10-CAP achieved an approximately 43% improvement in the data rate under the clear atmosphere condition. Further, for a 500 m-long 10-CAP hybrid FSO/VLC link under turbulence, the drops in R_b were 8.9% and 30% for C_n^2 of 3.9×10^{-17} m$^{-2/3}$ and 2.4×10^{-15} m$^{-2/3}$, respectively, compared to the link with no turbulence. It was also shown that, the effect of increasing m for higher turbulence levels did not lead to improvement in the measured R_b.

References

[1] Cisco, San Jose, CA, USA, "Cisco visual networking index: Global mobile data traffic forecast update, 2016–2021 white paper," 2018.

[2] Z. Ghassemlooy, W. Popoola, and S.Rajbhandari, *Optical Wireless Communications: System and Channel Modelling With MATLAB*. New York, NY, USA: Taylor & Francis, 2012.

[3] Z. Ghassemlooy, L. N. Alves, S. Zvanovec, and M-A. Khalighi, *Visible Light Communications: Theory and Applications*. Boca Raton, FL, USA: CRC Press, Jun. 2017.

[4] A. Paraskevopoulos, J. Vucic, S. H. Voss, R. Swoboda, and K. D. Langer, "Optical wireless communication systems in the Mb/s to Gb/s range, suitable for industrial applications," *IEEE/ASME Trans. Mechatronics*, vol. 15, no. 4, pp. 541–547, Aug. 2010.

[5] G. Parca, A. Shahpari, V. Carrozzo, G. M. T. Beleffi, and A. L. Teixeira, "Optical wireless transmission at 1.6-Tbit/s (16×100 Gbit/s) for next-generation convergent urban infrastructures," *Opt. Eng.*, vol. 52, no. 11, pp. 102–116, 2013.

[6] L. C. Andrews and R. L. Phillips, *Laser Beam Propagation Through Random Media*, 2nd ed. Washington, DC, USA: SPIE Press, 2005.

[7] S. Rajbhandari *et al.*, "A review of gallium nitride LEDs for multi-gigabit-per-second visible light data communications," *Semicond. Sci. Technol.*, vol. 32, no. 2, 2017, Art. no. 23001.

[8] H. Le Minh *et al.*, "High-speed visible light communications using multiple-resonant equalization," *IEEE Photon. Technol. Lett.*, vol. 20, no. 14, pp. 1243–1245, Jul. 2008.

[9] G. Cossu, A. M. Khalid, P. Choudhury, R. Corsini, and E. Ciaramella, "3.4 Gbit/s visible optical wireless transmission based on RGB LED," *Opt. Express*, vol. 20, no. 26, pp. 501–506, 2012.

[10] Z. Jia, L. Yuan, and H. Guo, "Visible light communication system based on multi-level pulse code modulation," in *Proc. 5th IEEE Int. Conf. Broadband Netw. Multimedia Technol.*, Guilin, 2013, pp. 222–226.

[11] R. X. G. Ferreira *et al.*, "High bandwidth GaN-based micro-LEDs for multi-Gb/s visible light communications," *IEEE Photon. Technol. Lett.*, vol. 28, no. 19, pp. 2023–2026, Oct. 1, 2016.

[12] D. Bykhovsky and S. Arnon, "An experimental comparison of different bit-and-power-allocation algorithms for DCO-OFDM," *J. Lightw. Technol.*, vol. 32, no. 8, pp. 1559–1564, Apr. 15, 2014.

[13] Z. Yu, R. J. Baxley, and G. T. Zhou, "Peak-to-average power ratio and illumination-to-communication efficiency considerations in visible light OFDM systems," in *Proc. IEEE Int. Conf. Acoust., Speech, Signal Process.*, Vancouver, BC, Canada, 2013, pp. 5397–5401.

[14] F. M. Wu *et al.*, "Performance comparison of OFDM signal and CAP signal over high capacity RGB-LED-based WDM visible light communication," *IEEE Photon. J.*, vol. 5, no. 4, Aug. 2013, Art. no. 7901507.

[15] M. I. Olmedo *et al.*, "Multiband carrierless amplitude phase modulation for high capacity optical data links," *J. Lightw. Technol.*, vol. 32, no. 4, pp. 798–804, Feb. 15, 2014.

[16] P. Chvojka, S. Zvanovec, K. Werfli, P. A. Haigh, and Z. Ghassemlooy, "Variable m-CAP for bandlimited visible light communications," in *Proc. IEEE Int. Conf. Commun. Workshops*, Paris, Italy, 2017, pp. 1–5.

[17] P. Chvojka *et al.*, "On the m-CAP performance with different pulse shaping filters parameters for visible light communications," *IEEE Photon. J.*, vol. 9, no. 5, Oct. 2017, Art. no. 7906712.

[18] Z. Huang *et al.*, "Hybrid optical wireless network for future SAGO-Integrated communication based on FSO/VLC heterogeneous interconnection," *IEEE Photon. J.*, vol. 9, no. 2, Apr. 2017, Art. no. 7902410.

[19] P. Chvojka, P. A. Haigh, S. Zvanovec, P. Pesek, and Z. Ghassemlooy, "Evaluation of multi-band carrier-less amplitude and phase modulation performance for VLC under various pulse shaping filter parameters," in *Proc. 13th Int. Joint Conf. e-Bus. Telecommun.*, Lisbon, Portugal, 2016, vol. 3, pp. 25–31.

[20] N. A. M. Nor *et al.*, "Experimental investigation of all-optical relay-assisted 10 Gb/s FSO link over the atmospheric turbulence channel," *J. Lightw. Technol.*, vol. 35, no. 1, pp. 45–53, Jan. 1, 2017.

[21] M. Amini Kashani, M. Uysal, and M. Kavehrad, "A novel statistical channel model for turbulence-induced fading in free-space optical systems," *J. Lightw. Technol.*, vol. 33, no. 11, pp. 2303–2312, Jun. 2015.

[22] L. C. Andrews, *Field Guide to Atmospheric Optics*. Washington, DC, USA: SPIE Press, 2004.

[23] H. Kaushal *et al.*, "Experimental study on beam wander under varying atmospheric turbulence conditions," *IEEE Photon. Technol. Lett*, vol. 23, no. 22, pp. 1691–1693, Nov. 2011.